Appl. Phys. B 61, 361–366 (1995)

Applied Physics B Lasers and Optics

Photoacoustic analysis of stimulated emission in pulsed dye lasers

M. Villagrán-Muniz[1], C. Garcia-Segundo[1], H.F. Ranea-Sandoval[2,*], C. Gogorza[2], G.M. Bilmes[3,]**

[1] Centro de Instrumentos, UNAM, Apdo. Postal 70-186, 04510 D.F. México, México
[2] Instituto de Física "Arroyo Seco", FCE-UNCPBA, Calle Pinto 399, 7000 Tandil, Argentina
[3] Centro de Investigaciones Opticas (CIOp) (CONICET-CICBA), Casilla de Correos 124, 1900 La Plata, Argentina
(Fax: + 54-21/71-2771, E-mail: POSTMASTER@ciop.edu.ar)

Received: 10 June 1994/Accepted: 30 January 1995

Abstract. Stimulated emission in pulsed dye lasers was characterized in several experimental conditions by analyzing the changes in the acoustic signals generated in a dye solution, with the dye laser cavity either active or inhibited (i.e., by blocking the optical path or misaligning of the optical components). Pump energy threshold, optimum dye concentration, tuning range and maximum-emission wavelength of a rhodamine 6G dye laser were measured by this method. An approximate model for the photoacoustic signal generation consistent with the experiments is presented.

PACS: 42.55. Mv; 82.80. Kq

The characterization of stimulated emission in a laser medium and particularly measurements of gain, energy threshold for laser emission, tunability and dependence with parameters as losses, temperature, concentration of species, and others, are usually performed by means of optical detection. In many cases the results are strongly dependent on the way in which the total light emitted is collected and there are some difficulties to recognize the contribution of spontaneous emission, amplified spontaneous emission (ASE) and laser emission.

Photoacoustic detection has proven useful to measure the energy dissipated as heat as a consequence of deactivation of excited states by non-radiative transitions [1, 2]. In this technique the heat is released to the medium intermittently (i.e. pulses), producing periodic contractions and expansions which generate acoustic signals.

In this work we present a new method for the characterization of stimulated emission in pulsed lasers based in photoacoustic detection. The main idea is to detect stimulated emission processes, measuring the changes produced in the acoustic signals generated in the laser medium, after excitation, in conditions of good laser cavity (active) or bad (inhibited) cavity. These changes are due to the competition, for the population inversion, between the stimulated emission and the other deactivation mechanisms.

As an example we show an application to the case of pulsed dye lasers, for which laser emission can be modified easily as a function of different parameters like pump energy, emission wavelength to which the cavity is tuned, dye concentration, alignment and losses (reflectivities of the mirrors or stray losses).

On the other hand, there is an additional interest in the characterization of the processes of generation and detection of acoustic signals in dye molecules, as it was shown to be a useful technique for the study of photophysical processes and for the determination of kinetic and other physical parameters of the molecules [3–5]. Under conditions for absorption and fluorescence spectroscopy (i.e. thin solutions and low fluences), the main radiative channel is spontaneous emission, while induced emission is highly unlikely to be detected. The question about the influence of stimulated emission may arise, since in many cases there is some necessity of knowing the rate for emission process, among other parameters. Interference with other phenomena not accounted for in the models used, can thus lead to erroneous evaluation of searched parameters.

We present here experiments and a model for a rhodamine 6G dye laser for which the stimulated emission process was detected via the changes in the photoacoustic signal, conveniently recorded in a system with similar characteristics to the one used in photoacoustic absorption spectroscopy analysis. The difference lies in the fact that the cell is placed in a laser cavity, and that the concentrations and the pump fluences are high enough to allow the laser onset. This method has proved to be not only good to test the limits of validity of the spectroscopic analysis done so far in this kind of molecules, but has also

* Member of CONICET
** To whom all correspondence should be addressed. Member of CIC-BA

provided good information about several parameters of interest to describe the performance of a dye laser.

1 Experimental set-up

Figure 1 shows the experimental set-up used. It uses basically a home-made Littrow mounting rhodamine 6G dye laser, pumped by the second harmonic of a Q-switched Nd^{+3}–YAG laser (Surelite I, Continuum). The pump beam was expanded (T) and then focused (L) into the dye cell. A piezoelectric ceramic transducer (4 × 4 mm), similar to the one used, for example, in [6], was attached to the lower part of the rear wall (in relation to the pump wall) of the dye cell in order to detect the photoacoustic signal. The amplitude H of the acoustic signal was amplified and processed by a storage digital oscilloscope (TDS 540, Tektronix) both for good and bad laser cavity conditions.

Pyroelectric and silicon detectors (RjP-765, RjP-735), Laser Precision) were used to determine the pump and dye laser energy.

2 Results and discussion

Due to the competition processes between stimulated emission and the other deactivation mechanisms, as will be shown in this section, photoacoustic signals for good laser cavity conditions are lower than the same signals in the bad cavity case. Their difference depends on the emission wavelength to which the cavity is tuned, the gain, the dye concentration, the alignment, the pump conditions, and the losses (reflectivities of the mirrors or stray losses). We studied the behaviour of the amplitude of the acoustic signals as a function of the above parameters and the alignment of the system [7].

In Fig. 2a the dependence of the pump-energy normalized amplitude of the first photoacoustic signal (H/E_p) is displayed as a function of the pump energy (E_p) in the active cavity and the inhibited cavity cases. Figure 2b shows the results for the theoretical model developed which qualitatively reproduces the same features of the experiment. The details of this model can be found in Sect. 3.

We define the "photoacoustic signal ratio" of the dye laser as the ratio between the amplitudes of the acoustic signal when the cavity is active (H_l) to the signal when the cavity is inhibited by blocking the mirror or the grating (H_{nl}), namely H_l/H_{nl}. Optical measurements were done for

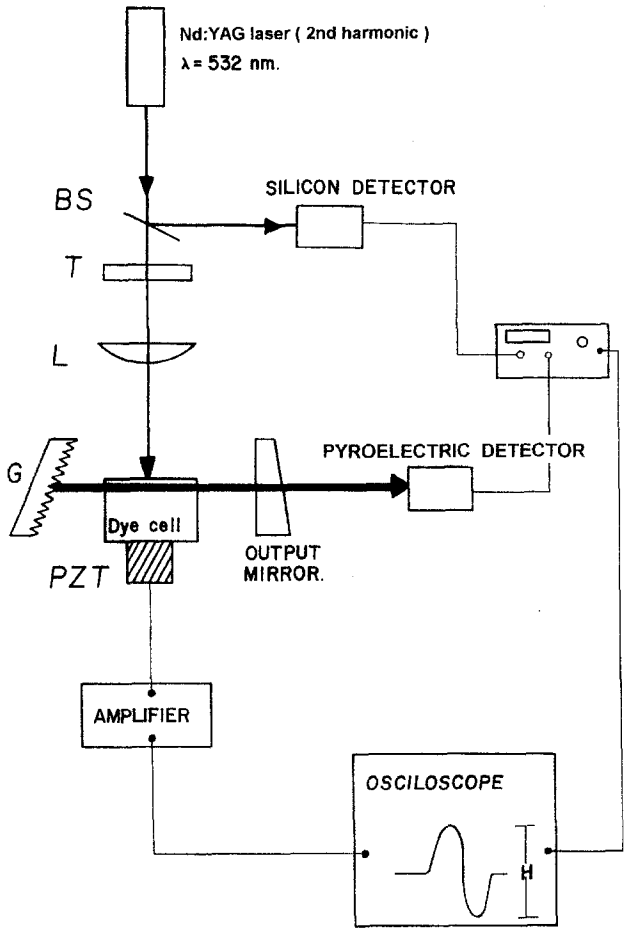

Fig. 1. Experimental set-up. *BS* Beam Splitter; *T* Telescope; *L* Cylindrical lens; *PZT* Piezoelectric detector; *G* Grating

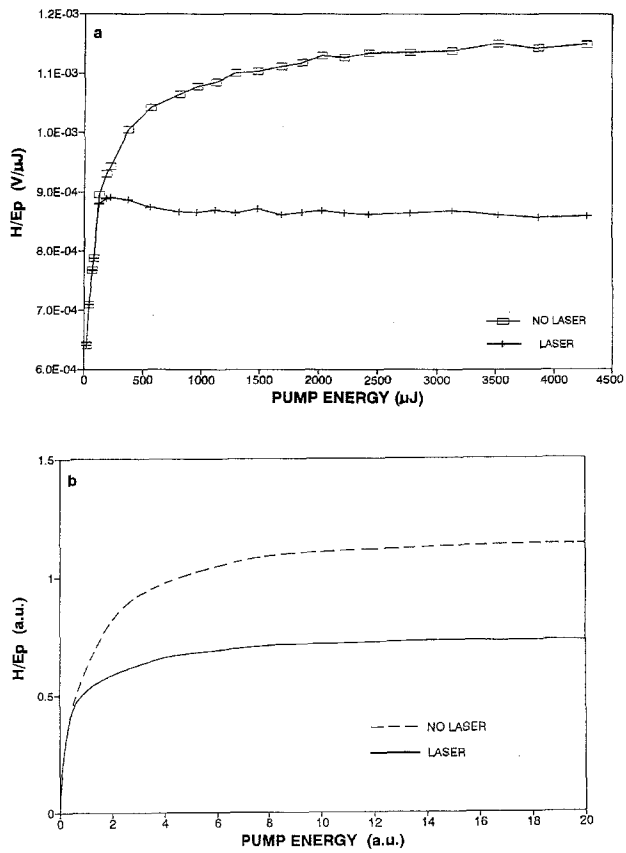

Fig. 2a, b. Experimental (**a**) and theoretical (**b**) energy dependence of the energy normalized amplitude of the first acoustic signal (H/E_p) for inhibited cavity (no laser H_{nl}), and active cavity (laser H_l). The laser onset is clearly visible in **a** at 200 μJ pump energy

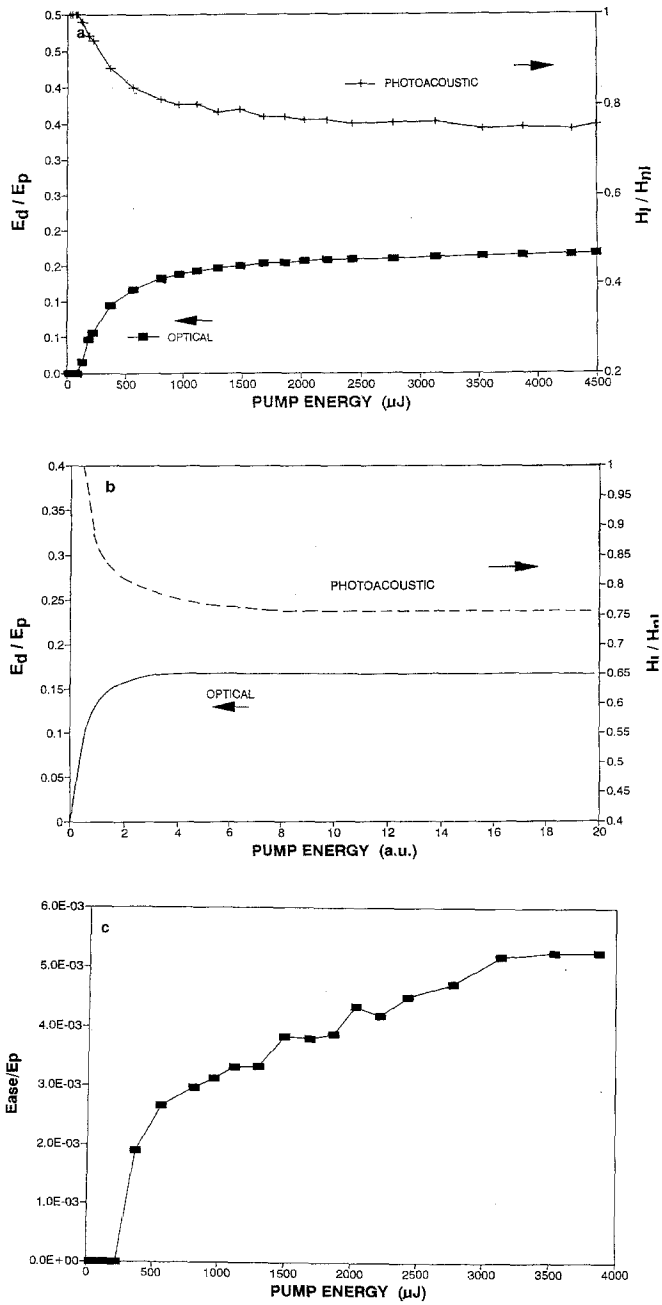

Fig. 3a–c. Experimental (**a**) and theoretical (**b**) energy dependence of the photoacoustic signal ratio (H_l/H_{nl}) and optical energy efficiency (E_d/E_p). **c** Is the pump energy normalized amplified spontaneous emission (E_{ase}/E_p) as a function of the pump energy

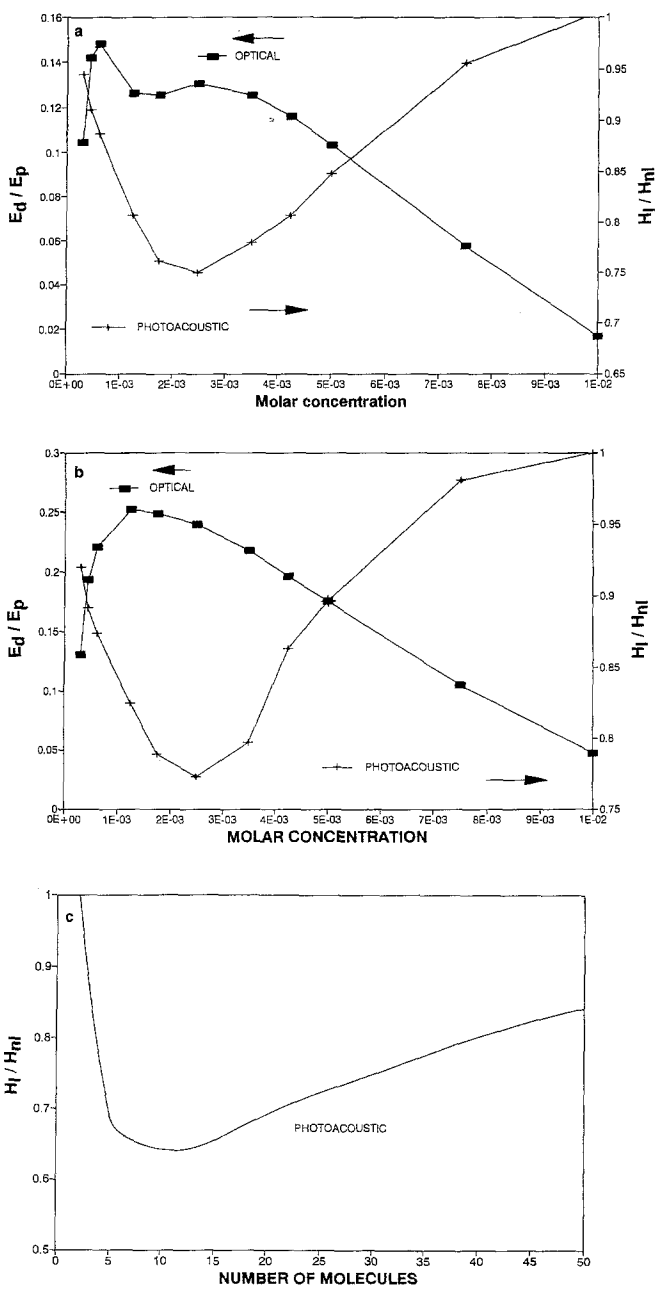

Fig. 4a–c. Photoacoustic signal ratio and optical energy efficiency as a function of the dye concentration. **a** E_d/E_p was measured collecting only the light at the centre of the beam. **b** E_d/E_p was measured collecting all the light emitted with a lens. **c** Is the result of the analytical model.

control in the same conditions, so we used the definition of "optical energy efficiency", E_d/E_p, as the ratio between the dye-laser output energy (E_d) to the pump energy (E_p). Figure 3a shows the energy dependence of the photoacoustic signal ratio and the optical efficiency of the laser. The threshold energy for laser onset was evaluated to be approximately 200 μJ.

Correspondingly, Fig. 3b is the result of the theoretical model for conditions similar to the one of Fig. 3a. Once again, the qualitative agreement is clearly displayed.

Dye lasers pumped with very high power densities are known to generate Amplified Spontaneous Emission (ASE). This is likely to affect the photoacoustic signal up to some extent; this is the reason why we characterize it in our set-up. The results of the experiment are displayed in Fig. 3c, where E_{ase}/E_p is the ASE energy output normalized to (E_p). Photoacoustic and optical measurements are displayed in Figs. 4a and b as functions of dye concentration (in EtOH), evaluated from experimental data. Optical efficiency depends on how the light from the laser is detected and this is important when ASE cannot be neglected. In fact, if a diaphragm is placed before the light

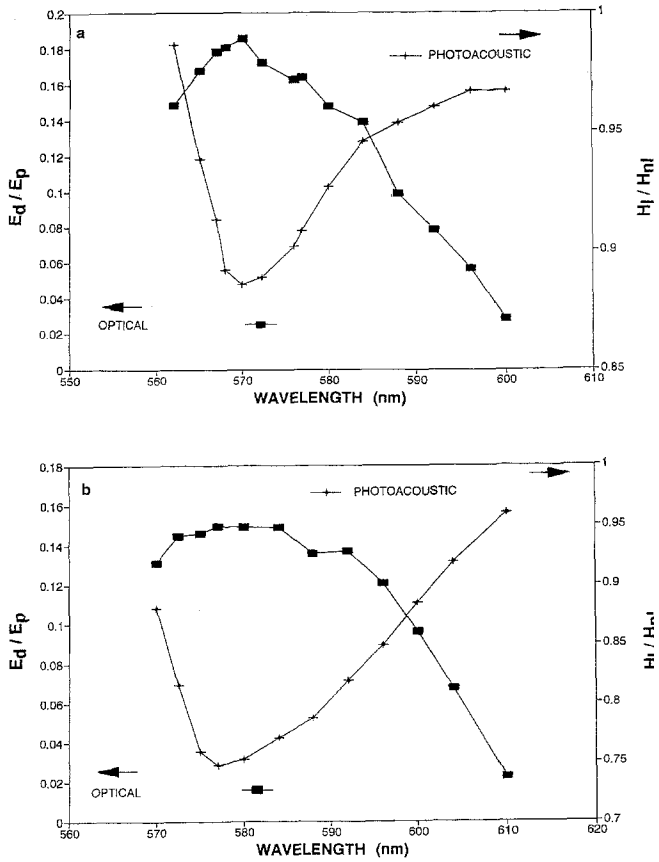

Fig. 5 a,b. Photoacoustic signal ratio and optical energy efficiency as a function of the tuning wavelength for two concentrations of the dye **a** 6.25×10^{-4} M and **b** 2.5×10^{-3} M

detector, considering only the central part of the laser beam, there is a concentration for which the optical efficiency is maximum around 6.25×10^{-4} M. Instead, when all the beam is considered, i.e. considering the total ASE, the optimum concentration is found to be 2.5×10^{-3} M. This value corresponds to the maximum photoacoustic signal ratio. The first concentration is approximately equal to the one recommended by the laser-grade dye manufacturer for optimum laser performance. In Fig. 4c, the results of the analytical model is displayed for comparison.

Figure 5a and b display H_l/H_{nl} and E_d/E_p as a function of the wavelength to which the laser is tuned for the above-mentioned concentrations. As expected, ASE is more important the higher the concentration.

When the photoacoustic signal ratio of Fig. 5 is normalized to the dye laser output energy, the results show that aside from minors effects, there is no experimental evidence of a specific dependence of H_l/H_{nl} with the wavelength, which is an evidence of the homogeneous broadening of the transition.

3 Analytical model

An approximate model for the photoacoustic signal generation in a laser medium was developed in order to establish the relative influence of several dynamical parameters and to analyze the competition processes among deactivation pathways.

The model consists in a simplified formulation for the photoacoustic signal generation for cavity inhibited or active. It is therefore necessary to determine all the stationary state populations in both cases and to assume a heat decay rate. In the case of an active cavity, this model uses the general consideration of a well-established semi-classical approach to the laser dynamics [8, 9] in order to evaluate the laser intensity, neglecting all spontaneously emitted light.

A very well-known energy scheme for an excited dye molecule is displayed in Fig. 6, where, the main deactivation processes are shown by which the ground state is reached. There are radiative and non-radiative channels. The latter are due to conversion of vibrorotational molecular energy into kinetic energy of the solvent molecules, and internal conversion process which drives the molecule from S_1 to S_0. The heat released by the excited molecule in each one of the above-described processes of this non-radiative deactivation are Q_2, Q_3 and Q_1, respectively. The radiative channels for the energy down conversion are spontaneous emission and induced emission.

When the cavity is inhibited, we represent the signal by the formula

$$H_{nl} \alpha [\sigma p(E_{exc} - E_1) N_{00} + \sum (E_n/r) N_{n0} + (1 - \phi) E_1 N_{10}], \quad (1a)$$

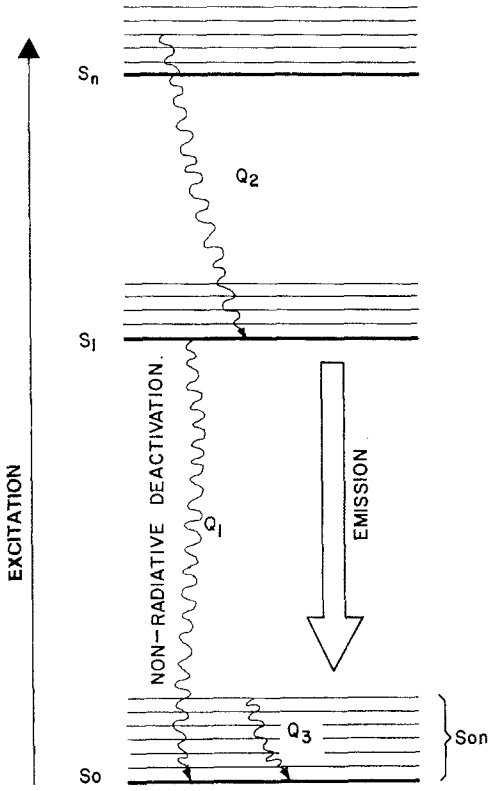

Fig. 6. Dye molecule excitation and deactivation pathways. Q_i, heat released by the excited molecule.

while, for an active cavity,

$$H_1 \alpha [\sigma p(E_{exc} - E_1) N_0 + \sum (E_n/r) N_n + (1 - \phi) E_1 N_1 + \rho H_{nl}], \quad (1b)$$

where σ is the absorption cross-section of excited states, p is the pump (i.e. number of photons per pulse); E_{exc}, E_1 and E_n are the energy content of the excitation pulse, of the principal transition from S_1 and of the transitions within the S_0 band, respectively; ϕ is the fluorescence quantum yield, and r is the ratio of the singlet deactivation time constant to the deactivation time constant of the S_{0n} levels (considered all equal). The sums represent the contribution of all sublevels to the radiated heat. On the other hand, N_0 is the population of the ground state from which the molecules are optically pumped, N_1 is the population of the bottom level of S_1, and N_n is the population of the n-th sublevel of $S_0(S_{0n})$. An extra zero has been added to these variables when they refer to the inhibited cavity case.

The terms in both equations are the contributions to the signal coming from the depopulation of the levels via non-radiative transitions. The first terms give the heat coming from excited levels other than the bottom of S_1, the second are due to the deactivation of the sublevels of the ground state, and finally, the third represents the radiationless depopulation of S_1. To H_1, then, a fourth term is added phenomenologically, which is the contribution to the signal from regions which are pumped, but are not involved in the laser process. Although the results are qualitatively independent of this percentage, the experimental results reveal that the heat coming from this region is an important source of interference between both measurements.

The evaluation of the acoustic signals requires the knowledge of the populations and rate constants, the latter coming from an analysis of the band, and the former from the dynamics of the system.

In our case, to evaluate the acoustic signal a simplified version of the energy level diagram and of the band structure is used, in which only the ground state is considered to have a band-like structure consisting of many sublevels. Also we assume that the excitation wavelength is tuned to the absorption of the bottom level of $S_1(E_{exc} = E_1)$, which means that $Q_2 = 0$.

For the case when the cavity is inhibited, the evaluation of the populations is made through a set of rate equations, giving for the stationary values,

$$N_{10} = \sigma_1 p N [1 + \sigma_1 p(r\phi + 1)]^{-1}, \quad (2a)$$

$$N_{n0} = \sigma_1 p r f_n N (1 + \delta_n^2)^{-1} [1 + \sigma_1 p(r\phi + 1)]^{-1} \quad (2b)$$

and

$$N_{00} = N [1 + \sigma_1 p(r\phi + 1)]^{-1}, \quad (2c)$$

where N is the total number of molecules,

$$N = N_{00} + N_{10} + \sum N_{n0} \quad (2d)$$

and the sum is extended to all the sublevels of the ground state which are populated by N_n molecules, respectively, σ_1 is the absorption cross-section of S_1.

In (2b) f_n are the dipole strengths of the transition $S_1 \rightarrow S_{0n}$ normalized so that

$$\sum f_n (1 + \delta_n^2)^{-1} = \phi. \quad (3a)$$

where Lorentzian lineshape is assumed and

$$f_n = M(1 + a^2 \delta_n^2)^{-1}. \quad (3b)$$

In (3), δ_n is the energy difference between the n-th sublevel from the ground state (in non-dimensional units) and a is the ratio of the inhomogeneous width to the homogeneous one (Γ_p/Γ).

In order to consider the laser influence on the populations of the levels, we use the semi-classical approach, and in this frame, the set of equations for the steady state, give the following results:

$$N_1 = \sigma_1 p N_0 - I/r, \quad (4a)$$

$$N_n = I f_n (1 + \delta_n^2 + f_n I)^{-1} \quad (4b)$$

Again

$$N = N_0 + N_1 + \sum N_n \quad (4c)$$

The laser intensity, I, is evaluated from the condition

$$\sum f_n (N_1 - N_n)(1 + \delta_n^2)^{-1} = 1 \quad (5)$$

in a linear approximation.

The model for the laser operation, in its original form, did not contain any information regarding a possible depletion of the ground state due to the relaxation time of the vibrorotational states of the ground level. Here we include this effect in a form of particle conservation equation. This model cannot include any effect referred to ASE.

Analytical photoacoustic signals are evaluated normalized to the absorbed pump energy and to the lifetime of the S_1 level. The laser dynamical variables and the pump p are normalized to the threshold values. For the parameters of rhodamine 6G included in the model we use $a = 0.1$, $\phi = 0.9$ and $r = 0.01$ with $N = 100$. Under these conditions analytical results are in qualitative agreement with the experimental data, as shown by the curves above. It can also be said that the modelled laser intensity is consistent with the measured one in the linear region, and with the linear part of the resulting intensity in [8, 9].

Figure 7 displays the excited singlet state population as evaluated from the model with the inhibited cavity and with the active cavity. A comparison between this figure and the figures with experimental data (see, for example, Fig. 2) show that the above-mentioned excited state population competition seems to be the mechanism responsible for the measured differences. Since this is related to the laser buildup, it means that with certain care it should be possible to devise a method for gain measurements.

In fact, the results obtained with the model are qualitatively the same as the experimental ones, even though absolute values and other details do not fit it. The main reason for this is that the model neither takes into account the contribution of ASE to the signal (which is known to be of some importance) nor the reabsorption of radiation, which is relevant at high concentrations. Since the laser intensity cannot be evaluated by this model under such conditions, no effort has been made in this direction whatsoever.

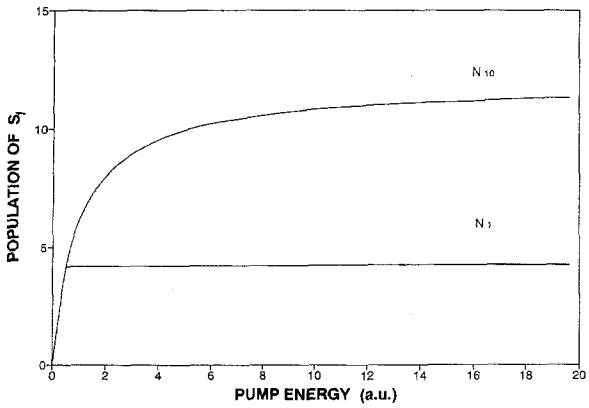

Fig. 7. Excited state population as evaluated from the model. The competition for this population happens to be the main channel for signal differences between the active and the inhibited cavity cases. For comparison, refer to Fig. 2a

The model also explains the reason why these measurements give no reliable results using a nitrogen laser pumped dye laser, due to the interference of the higher excited states deactivation heat.

4 Conclusions

The method hereby presented provides a test for the influence of stimulated emission on the population inversion of the laser medium, and enables full characterization of the laser through the parameter H_1/H_{n1}.

Good correlation between photoacoustic and optical data was found showing that with the former method there are some advantages due to its simplicity, high signal-to-noise ratio and sensitivity. Moreover, precise determination of the relationship between radiative and non-radiative deactivation mechanism can test in real time the efficiency of the dye and the influence of its photo physical parameters. On the other hand, it can be used to measure its chemical degradation.

The present model explain most of the experimental features observed and can be used to simulate the case of a UV pumped-dye laser, or a broad-band pumped one.

In fact, the heat generation in these two cases is high enough so as to obscure the reduction of the photoacoustical signal due to the laser action.

The dependence of the ratio between the two photoacoustical signals on the tuning frequency of the laser, when normalized to the laser energy, gives a precise measurement of the tuning range, and also good information about the wavelength for maximum output.

Photoacoustic detection can also be suitable for lasers with emission falling out of the visible range of the spectrum and for the characterization of vibronic lasers (Ti-sapphire), or alignment and optimization of non-fluorescent frequency converters.

Acknowledgements. We thank J.O. Tocho for fruitful discussions and comments during the preparation of the manuscript. Work partially supported by Projects CONACYT 1648-A9209, DGAPA-UNAM IN103692 (México) and BIDPID 0149 (Argentina).

References

1. A.C. Tam: In *Ultrasensitive Laser Spectroscopy Q.E. Principles and Applications*, ed. by D.S. Kliger (Academic, New York 1983) pp. 1–108
2. S.E. Braslavsky, G.E. Heibel: Chem Rev. **92,** 1381 (1992)
3. G.M. Bilmes, J.O. Tocho, S.E. Braslavsky: Chem. Phys. Lett. **134,** 335 (1987)
4. G.M. Bilmes, J.O. Tocho, S.E. Braslavsky: J. Phys. Chem. **92,** 5958 (1988)
5. G.M. Bilmes, J.O. Tocho, S.E. Braslavsky: J. Phys. Chem. **93,** 6696 (1989)
6. A.C. Tam, C.K.N. Patel: Opt. Lett. **5,** 27 (1980)
7. M. Villagrán-Muniz, C. Garcia-Segundo, H.F. Ranea-Sandoval, G.M. Bilmes: In *Tech. Dig. 8th Int'l Topical Meeting on Photoacoustic and Photothermal Phenomena* (1994) Paper BP-27, p. 67
8. H. Fu, H. Haken: Phys. Rev. **36,** 3032 (1987)
9. H. Fu, H. Haken: J. Opt. Soc. Am. B **5,** 899 (1988)